Electrochemical Performance and Surface Properties of Bare and TiO_2-Coated Cathode Materials in Lithium-Ion Batteries

Zhongru Zhang, Zhengliang Gong, and Yong Yang*

State Key Laboratory for Physical Chemistry of Solid Surfaces and Department of Chemistry, Xiamen University, Xiamen, 361005, P.R. China

Received: July 8, 2004; In Final Form: August 17, 2004

Electrochemical performance and spectroscopic characterizations of the decomposition products from electrolytes on native and TiO_2-coated $LiCoO_2$ and $LiMn_2O_4$ in different potential regions were investigated. The results showed that TiO_2-coated materials exhibited better cyclic stability in different potential regions (i.e., 3.0−4.3 V and 3.0−4.6 V), and the decomposition of the electrolytes was suppressed on the coated materials surface. Results from FTIR and temperature-programmed-desorption mass spectroscopy (TPD-MS) showed that the decomposition of the electrolytes on the electrode surface is related to both the material measured and the oxidation potential. The causes for the formation of different oxidation products of electrolytes have been analyzed. An improved electrooxidation mechanism of the electrolytes was also proposed. It is shown that the different reactivity of cathode materials to the oxidation of electrolytes can well be related to their thermal stability in practical Li-ion batteries.

Introduction

As high capacity cathodes for lithium-ion batteries, lithium transition-metal oxides and their derivatives, such as $LiCoO_2$, $LiMn_2O_4$, $LiNi_{0.8}Co_{0.2}O_2$, and so on, have been studied extensively.[1−5] To optimize cathode performance, differently modified electrode materials have been reported in the literature.[6−11] However, optimization of an electrode material is only the first step in the process leading to its implementation in a practical cell. Indeed, the electrochemical performance and thermal stability of electrode materials are closely related to reactions occurring on electrode−electrolyte interfaces.[12]

Many studies have indicated that surface coating is generally beneficial for improving the performance of the electrode material.[13−16] However, the mechanism of improved material performance generated by coating is still not clear. Some groups suggested[16,17] that the improvement may be related to the depression of some side reactions, including the oxidation of electrolytes on the electrode surface, but they did not give direct experimental evidence. Previous studies[18,19] from our laboratory showed that different oxidation products were formed on the $LiNi_{0.8}Co_{0.2}O_2$ electrode surface as monitored by Fourier transform infrared (FTIR) and temperature-programmed desorption mass spectrometry (TPD-MS) spectroscopic techniques; for them, a possible electrooxidation mechanism of the electrolytes has been proposed. It has also been demonstrated that there exists some strong interactions between electrode materials and oxidation products.

Safety is one of the most important issues in the development and application of Li-ion batteries. It mainly relates to the thermal reactions of components in batteries (i.e., the thermal decomposition of the electrode materials and electrolytes, etc.), whereas the reaction between the electrodes and electrolytes is a major part of the thermal reaction of the components. For example, it is proven that the thermal stability of cathode materials is on the order of $LiMn_2O_4$ > $LiCoO_2$ > $LiNi_{0.8}Co_{0.2}O_2$.[20−22] Therefore, it is helpful to understand the thermal stability of batteries through the study of the decomposition of electrolytes on the electrode surface and the effect on thermal reactions between electrolytes and electrode materials.

TPD-MS is frequently applied to obtain the mass−electric charge ratio (*m*/*e*) of adsorbed species in the catalysis research field; FTIR is a powerful technique to characterize the functional groups of the adsorbed species on the surface of electrodes. A combination of the two techniques should confidently determine the species adsorbed on the electrode surface.

In this work, $LiCoO_2$ and $LiMn_2O_4$ particles were coated with a thin surface layer of TiO_2 by a chemical method. Their electrochemical performance and surface organic species were investigated by microelectrode and FTIR techniques. Furthermore, the TPD-MS technique was applied to analyze the decomposition products of the electrolyte on the cathode material surface. On the basis of our electrochemical and spectroscopic results, the causes for the formation of different oxidation products were analyzed. On the basis of the previous study, as well as the present results, the correlation between electrode reactivity for the electrolyte decomposition and thermal behavior of the electrode materials was determineed.

Experimental Section

Materials. $LiCoO_2$ and $LiMn_2O_4$ were purchased from Merck Corporation, and the corresponding TiO_2-coated powders were synthesized by the hydroxylation of tetra-*n*-butyl titanate (TBT) in air; the resulting mole ratio of Ti is 3%. The sintering condition was controlled at 400 °C for 5 h in air. The thickness of the coating layer was approximately 20−35 nm measured by means of scanning electron microscopy (SEM) and transmission electron microscopy (TEM) imaging.[18−19]

* To whom all correspondence should be addressed. Phone: 086-0592-2185753. Fax: 086-0592-2185753. E-mail: yyang@xmu.edu.cn.

10.1021/jp046980h CCC: $27.50
Published on Web 10/15/2004

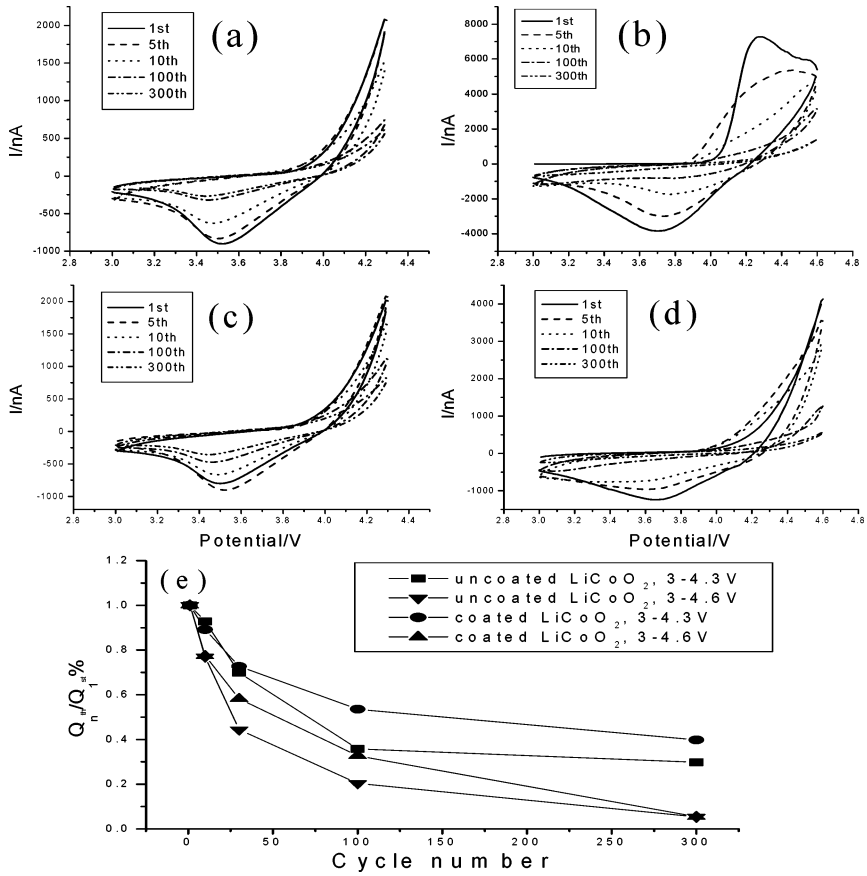

Figure 1. Cyclic voltammograms of $LiCoO_2$ with and without TiO_2 coating at 10 mV/s in 1 M $LiPF_6$/EC + DMC (1:1) in different potential regions: (a) uncoated $LiCoO_2$, 3.0−4.3 V, (b) uncoated $LiCoO_2$, 3.0−4.6 V, (c) TiO_2-coated $LiCoO_2$, 3.0−4.3 V, (d) TiO_2-coated $LiCoO_2$, 3.0−4.6 V, (e) relative changes in discharge capacities of the uncoated and TiO_2-coated $LiCoO_2$ particles during CV cycles.

Methods. Cavity powder microelectrodes (CMEs) were made of a glass tube containing a Pt wire (diameter, 100 μm) inside; the usual height−diameter of the cavity ratio was between 0.4 and 0.8.

The electrochemical experiments of the CMEs adopted three electrode systems and were performed using a CHI 600A potentiostat/galvanostat system (Shanghai, China). A Li foil pressed into a Ni net served as the counterelectrode and reference electrode. The electrolyte was 1 M $LiPF_6$/EC + DMC (1:1). The potential scan rate was 10 mV/s in the cyclic voltammety (CV) experiment. The ac impedance was measured after the CV scan completed, and the system was stabilized for 1−2 h. The cathode potential was set at 3.2 V during the measurement, which is close to the open circuit potential of the microelectrode. The ac perturbation signal was ±5 mV, and the frequency range was from 1 Hz to 10^4 Hz in the impedance experiments.

All FTIR measurements of electrodes were carried out by using a micro-IR spectrometer (Nicolet AVATAR 360 + Centaurμs IR Microscope, U.S.A.). The electrodes after cycling were washed immediately with DMC and dried in a glovebox for 24 h. The spectral resolution was set at 2 cm^{-1}, and all spectra were collected by 128 scans in all of the IR experiments.

TPD-MS experiments were performed by Qminstar QMS 200 (U.S.A.). First, the cathode materials were pressed directly onto Al foil, the electrodes were treated by two different methods, including the 300-cycle CV experiments and the potentiostatic oxidation experiments (the electrodes were potentiostatically oxidized until the current was less than 10 μA at different potentials), and then the electrodes were disassembled in the glovebox, washed with DMC, and placed in the box for 24 h to evaporate the liquid electrolyte. Finally, the powders were scraped from the Al foil and used for the TPD-MS experiments. Helium was the loading gas, the collection time of each channel was 0.1 s, and the rate of temperature increase was controlled at 15 °C/min.

Results and Discussion

Figures 1 and 2 show multicyclic voltammograms at 10 mV/s of $LiCoO_2$ and $LiMn_2O_4$, respectively, with and without TiO_2-coating on microelectrodes. Relative changes in discharge capacities against the number of CV cycles are also presented. It is apparent that all of the coated electrodes, especially that of $LiMn_2O_4$, exhibit better cycle stability in different potential regions. Even in the range of 3.0−4.6 V, the retention ratio of the discharge capacity is also above 80% after 300cycles. It is surprising that the cyclic performance of the $LiCoO_2$ electrode is much poorer in the range of 3.0−4.6 V, with or without coating. This degradation should be related to the structural destruction of the $LiCoO_2$ cathode materials and the formation of surface film. The formation of surface film may be caused by the two factors: (1) the decomposition of the electrolytes at a high potential. Aurbach and co-workers reported an oxidation potential below 4 V for $LiPF_6$/EC + DMC (1:1) electrolytes using Pt, Au, and Al as electrodes,[23] whereas the scan potential is much higher in our CV experiments. So, the decomposition of the electrolytes should be more serious. (2) The electrolytes are oxidized by the loss of oxygen from the $LiCoO_2$ cathode.[16,24−25] For the $LiCoO_2$ electrodes, it is thought that the second process is more important in our system. In TiO_2-coated $LiMn_2O_4$ at 4.6 V, but not with the uncoated material, a plateau current was

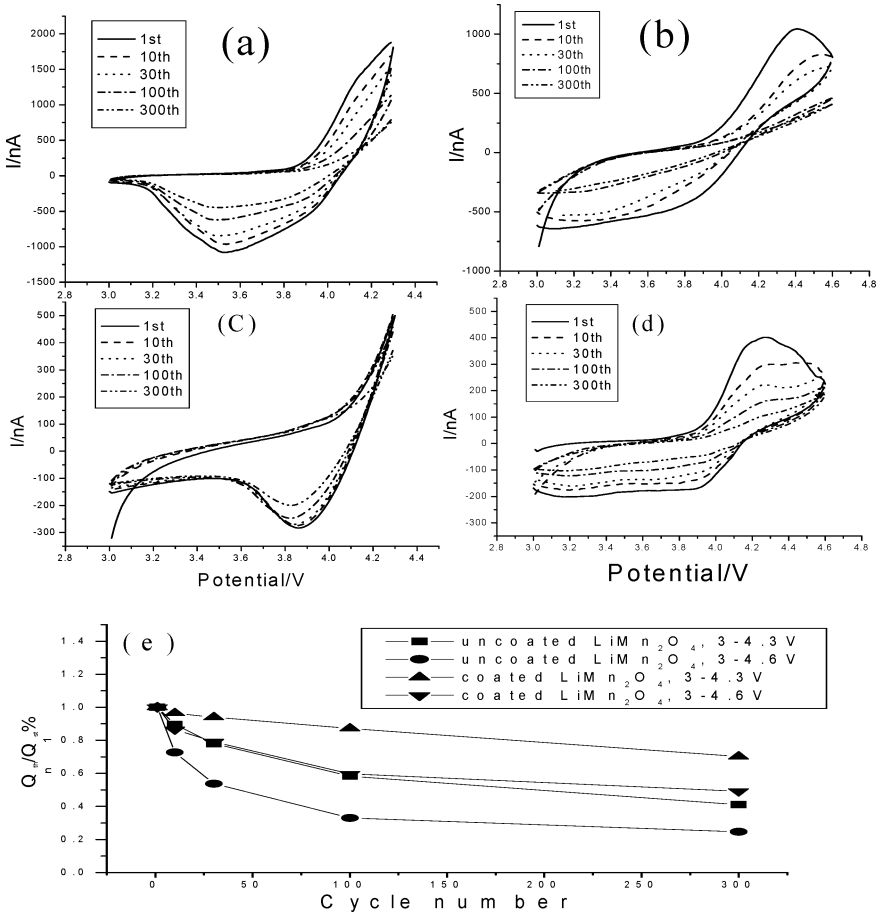

Figure 2. Cyclic voltammograms of $LiMn_2O_4$ with and without TiO_2 coating at 10 mV/s in 1 M $LiPF_6$/EC + DMC (1:1) in different potential regions: (a) uncoated $LiMn_2O_4$, 3.0−4.3 V, (b) uncoated $LiMn_2O_4$, 3.0−4.6 V, (c) TiO_2-coated $LiMn_2O_4$, 3.0−4.3 V, (d) TiO_2-coated $LiMn_2O_4$, 3.0−4.6 V, (e) relative changes in discharge capacity of the uncoated and TiO_2-coated $LiMn_2O_4$ particles during CV cycles.

observed in the reversing scan; this had not been reported in the literature as far as we know. The limited current plateau is probably caused by a slowdown in the Li^+ diffusion rate through the coated layer. In addition, after 300 cycles, the shapes of the CV curves in either coated or uncoated electrode materials have become different from those of the first cycle; the change is especially significant in the uncoated materials. This may imply that the charge-transfer resistance of these electrodes has greatly increased after long potential cycling.

Figures 3 and 4 compare electrochemical impedance spectroscopy (EIS) profiles of various electrodes before and after cycling at 10 mV/s in different potential regions. Normally, the initial real part of the impedance varies depending on both the materials used and the depth of microcavities in the microelectrodes. In addition, a high-frequency arc can be attributed to a charge-transfer process occurring at the electrode/electrolyte interface;[26,27] its changes should partially reflect the growth of a passive surface film formed by reactions between lithiated metal oxides and electrolytes. As shown in Figures 3 and 4, EIS profiles of all the electrodes exhibit a similar trend. All high-frequency arcs are increasing with the procession of CV experiments. When the potential was controlled in the range of 3.0−4.3 V, the arcs changed a little for the uncoated and coated materials. However, when the potential was increased to 4.6 V, changes became apparent. Furthermore, changes for the uncoated electrodes were much sharper than those for the coated electrodes. This may be explained by the fact that surface film formations are restrained, and the decomposition of electrolytes is suppressed at higher potentials on the TiO_2-coated material surface.

FTIR spectra of the coated and uncoated materials in the microcavity before and after 300 cycles in different potential regions are shown in Figures 5 and 6. New bands at approximately 1513 cm^{-1} (for $LiCoO_2$ material, see Figure 5) and 1510 cm^{-1} (for $LiMn_2O_4$ material, see Figure 6) are observed after electrochemical cycles. Both peaks can be assigned to the RCO_2^- stretching vibrations,[28,29] which indicate decomposition products in these electrochemical experiments that are mainly carboxylate salts, RCO_2^-. In addition, as seen in Figures 5 and 6, the intensity of this band for the uncoated electrode is greater than that of the coated electrode and increases dramatically with the cyclic potential. All of them indicate that the decomposition of electrolytes on uncoated electrode surfaces and at high potentials is much more serious, leading to more decomposition products. Meanwhile, it is found that the intensity of the 1510-cm^{-1} band for the Mn-based materials is much weaker than that for the Co-based materials under the same experimental conditions (including cyclic potential and coating modes); this also implies that the decomposition of the electrolytes on the Co-based electrode surfaces is more serious than that on Mn-based materials.

To further investigate these decomposition products, TPD-MS experiments after 300 cycles in different potential regions on various electrodes were performed. The mass/electron ratios (m/e) and corresponding assignments of the decomposition products are listed in Table 1. For comparison, the TPD-MS results of the $LiNi_{0.8}Co_{0.2}O_2$ electrodes from our previous paper are also included here.[18,19] It is found that the decomposition of the electrolytes is closely related to the intrinsic properties of the materials (i.e., the composition of transition-metal ions,

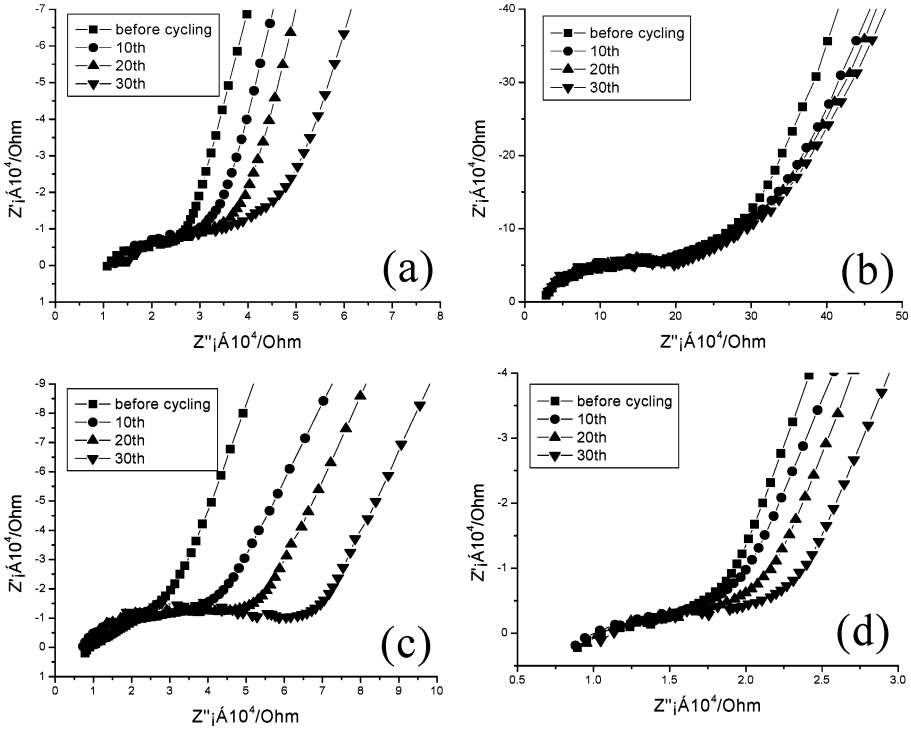

Figure 3. The ac impedance spectra of $LiCoO_2$ before and after multiple cycling at 10 mV/s in 1 M $LiPF_6$/EC + DMC (1:1): (a) uncoated $LiCoO_2$, 3.0−4.3 V, (b) TiO_2-coated $LiCoO_2$, 3.0−4.3 V, (c) uncoated $LiCoO_2$, 3.0−4.6 V, (d) TiO_2-coated $LiCoO_2$, 3.0−4.6 V.

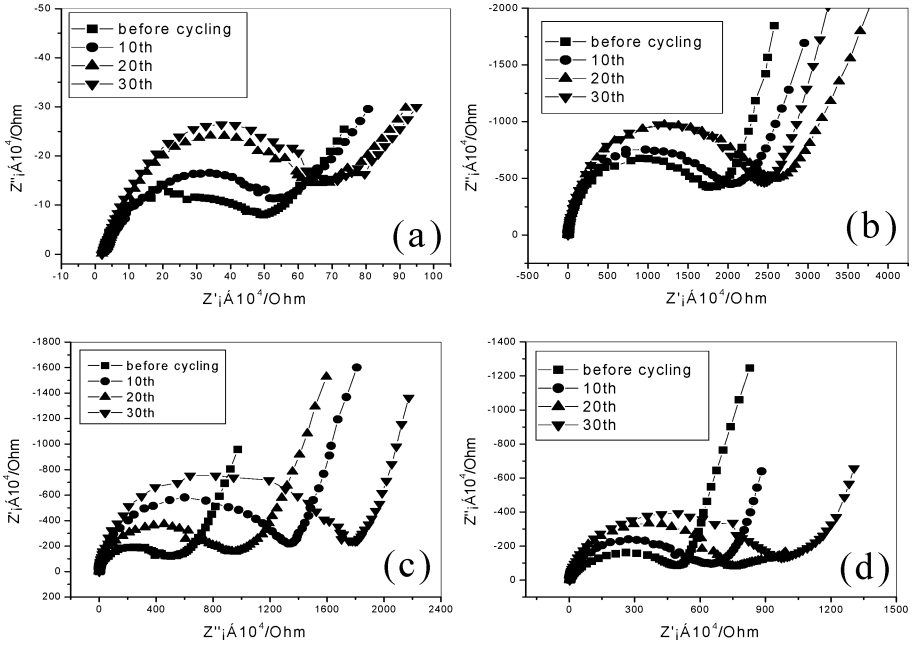

Figure 4. The ac impedance spectra of $LiMn_2O_4$ before and after multiple cycling at 10 mV/s in 1 M $LiPF_6$/EC + DMC (1:1): (a) uncoated $LiMn_2O_4$, 3.0−4.3 V, (b) TiO_2-coated $LiMn_2O_4$, 3.0−4.3 V, (c) uncoated $LiMn_2O_4$, 3.0−4.6 V, (d) TiO_2-coated $LiMn_2O_4$, 3.0−4.6 V.

the valence state of ions). The decomposition products are different on various electrode surfaces, even under the same experimental conditions. These experimental observations can be explained by two factors as stated here:

(1) the oxidative ability of transition-metal ions with high oxidation states. Generally, at a high potential (e.g., 4.6 V), lithium was extracted from the electrode materials, and these transition-metal ions were oxidized to a high oxidation state, such as to CoO_2, $Ni_{1-y}Co_yO_2$, and MnO_2, on the assumption that lithium was extracted completely and oxygen was not lost. It is well-known that MnO_2 has little oxidative ability, whereas $Ni_{1-y}Co_yO_2$ and CoO_2 are strong oxidants. Therefore, the decomposition of electrolytes on the $LiMn_2O_4$ electrode surface is weak but becomes stronger on the $LiNi_{1-y}Co_yO_2$ or $LiCoO_2$ electrode surface. In fact, lattice oxygen is lost from the $Li_{1-x}Ni_{1-y}Co_yO_2$ or $Li_{1-x}CoO_2$ surface,[24,25] and materials are transformed into formulations of nonstoichiometric compounds, such as $Li_{1-x}Ni_{1-y}Co_yO_{2-\delta}$ and $Li_{1-x}CoO_{2-\delta}$ with a low lithium content. Furthermore, more oxygen may be lost from the $Li_{1-x}CoO_{2-\delta}$ surface at the same lithium content, resulting in the actual oxidation state of Co in $Li_{1-x}CoO_{2-\delta}$ becoming lower than that of $Ni_{1-y}Co_y$ at $Li_{1-x}Ni_{1-y}Co_yO_{2-\delta}$. For example, Co in the $Li_{1-x}CoO_{2-\delta}$ surface has an oxidation state of only 3.34^+ and $\delta = 0.33$ with $x = 1$, whereas the average oxidation state

TABLE 1: Mass/Electron Ratio (*m*/*e*) and Corresponding Assignment of the Decomposition Products on Various Electrode Surfaces

	m/*e* assignment		30 HCHO	32 O_2 or CH_3OH	44 CO_2 or CH_3CHO	46 CH_3OCH_3	45 $HCOO^-$	59 CH_3COO^-	73 C_2H_5COO-	87 C_3H_7COO-
$LiCoO_2$	4.3V	uncoated	+[b]	+	+	+	+	□[c]	□	□
		coated	+	+	+	+	□	□	□	□
	4.6V	uncoated	+	+	+	+	+	□	□	□
		coated	+	+	+	+	+	□	□	□
$LiMn_2O_4$	4.3V	uncoated	+	+	+	+	□	□	□	□
		coated	+	+	+	+	□	□	□	□
	4.6V	uncoated	+	+	+	+	+	□	□	□
		coated	+	+	+	+	□	□	□	□
$LiNi_{0.8}Co_{0.2}O_2$[a]	4.3V	uncoated	+	+	+	+	+	□	□	□
		coated	+	+	+	+	+	□	□	□
	4.6V	uncoated	+	+	+	+	+	+	+	+
		coated	+	+	+	+	+	□	□	+

[a] Data intercept from ref 18. [b] + represents the presence of the species. [c] □ represents the absence of the species.

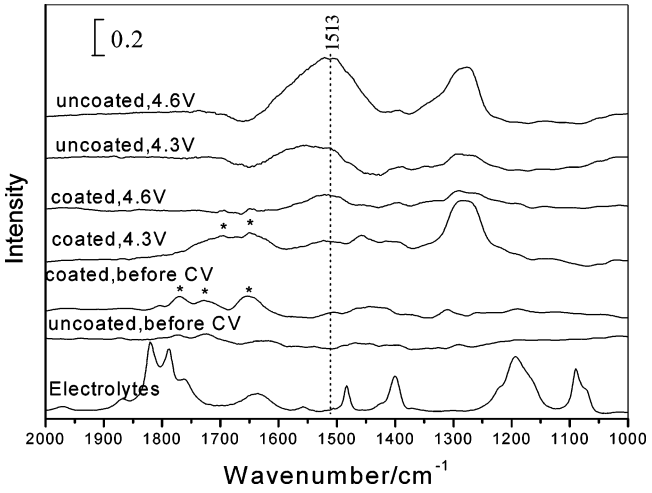

Figure 5. FTIR spectra of the uncoated and TiO_2-coated $LiCoO_2$ before and after 300 cycles in 1 M $LiPF_6$/EC + DMC (1:1) (* peaks represent the residual electrolyte). The conditions of the samples have been indicated above each spectrum.

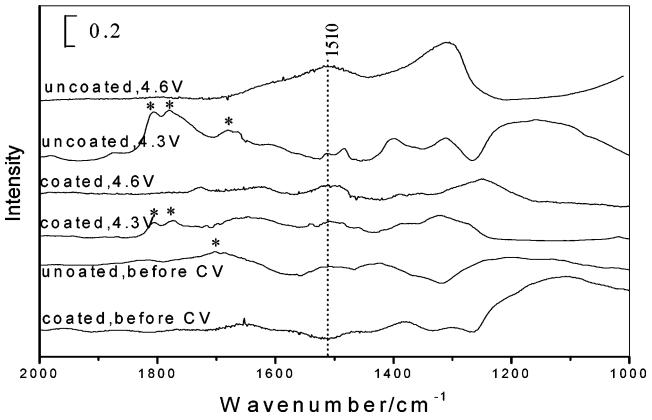

Figure 6. FTIR spectra of the uncoated and TiO_2-coated $LiMn_2O_4$ before and after 300 cycles in 1 M $LiPF_6$/EC + DMC (1:1) (* peaks represent the residual electrolyte). The conditions of the samples have been indicated above each spectrum.

of $Ni_{1-y}Co_y$ in the $Li_{1-x}Ni_{1-y}Co_yO_{2-\delta}$ surface is 3.8^+ and $\delta = 0.1$ with $x = 1$.[24,25] Furthermore, at the same potential, the amount of lithium extracted from $Li_{1-x}Ni_{1-y}Co_yO_{2-\delta}$ is larger than that from $Li_{1-x}CoO_{2-\delta}$. These factors make $Ni_{1-y}Co_yO_{2-\delta}$ a stronger oxidant than $CoO_{2-\delta}$.

(2) the catalytic properties of these transition-metal oxides. Nickel ions are very active catalysts for the alcohol oxidation reaction.[30] It was also reported that nickel[31] and nickel oxide electrodes[32] have good chemical catalytic, as well as electrocatalytic, properties for alcohol oxidation reactions. In comparison, cobalt ions have only chemical catalytic activity without electrocatalytic properties.[33,34] In contrast, catalytic properties for the alcohol oxidation of manganese ion have not been reported.

Whatever the reason for oxidative abilities or catalytic effects of electrode materials, it is necessary that the electrolytes be in contact with the electrode surfaces for the occurrence of electrochemical reactions; coating of materials may just prevent the reactions between these metal ions in the electrodes and the electrolytes, leading to the amount of electrolyte decomposition products being greatly reduced. Because of the detection limit of the MS instrument (ion current $> 10^{-14}$ A), the amount of decomposition products on some electrodes is too small to be detected in TPD-MS experiments. For example, those species on the $LiMn_2O_4$ electrodes at lower potential could not be detected in our experiments, whereas the carboxylate salts were still detected in FTIR experiments.

In addition, decomposition of the electrolytes is also related to the cyclic potential, as shown in Table 1. It shows that the higher the potentials are at the cathodic end, the larger the amount of the decomposition products. To investigate the composition and distribution of the decomposition products and to understand the relationship between electrolyte decomposition and oxidation potentials, TPD-MS experiments of various cathode materials after potentiostatic oxidation at different potentials (4.3 or 4.6 V) were performed, and measurements of *m*/*e* 30 and 45 are shown in Figure 7. There are some differences for $HCOO^-$ (*m*/*e* = 45), as shown in Figure 7 and Table 1. For example, the amount of species of *m*/*e* = 45 on $LiMn_2O_4$ electrodes is too small to be detected when the potentiostatic oxidation potential is set at 4.3 V. As shown in Figure 7, for HCHO (*m*/*e* = 30), the peak areas of curves a and c (the upper oxidation potential is 4.6 V) are always bigger than those of curves b and d (the upper oxidation potential is 4.3 V) on the same materials irrespective of the presence or absence of coating. These results indicate that the amount of HCHO (*m*/*e* = 30) from decomposition at the high potential is larger than at the low potential (i.e., determined by the oxidation potential). Normally, the amount of HCHO is different for different electrode materials. It is always largest on $LiNi_{0.8}Co_{0.2}O_2$ electrodes and smallest on $LiMn_2O_4$. These facts indicate that the yield of HCHO is determined not only by materials but also by oxidation potential.

In comparison to HCHO, the amount of $HCOO^-$ (*m*/*e* = 45) is scarcely related to the oxidation potential. For example, the peak areas of curve b (the oxidation potential at 4.3 V) are even

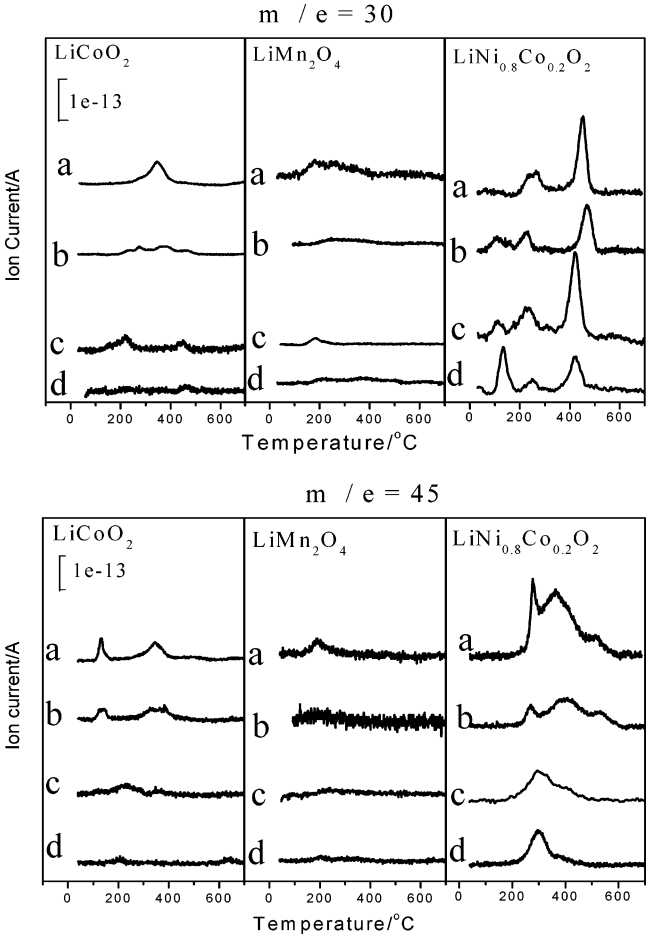

Figure 7. The TPD-MS spectra of various cathode materials after potentionstatic oxidation at different potentials in 1 M $LiPF_6$/EC + DMC (1:1): (a) uncoated, 4.6 V, (b) uncoated, 4.3 V, (c) TiO_2-coated, 4.6 V, (d) TiO_2-coated, 4.3 V.

larger than those of curve c (the oxidation potential at 4.6 V) for $LiCoO_2$ and $LiNi_{0.8}Co_{0.2}O_2$ electrodes, respectively, as shown in Figure 7. Furthermore, it should be noted that the peak areas of uncoated electrodes (curve a or b) are always larger than those of coated electrodes (curve c or d) at the same oxidation potential. Those results imply that the yield of $HCOO^-$ is mainly related to the oxidation properties of transition-metal ions and the modification of electrode surfaces.

In earlier reports,[18] we had studied the decomposition of the electrolytes on various $LiNi_{0.8}Co_{0.2}O_2$ material surfaces in detail and proposed a possible decomposition mechanism as follows

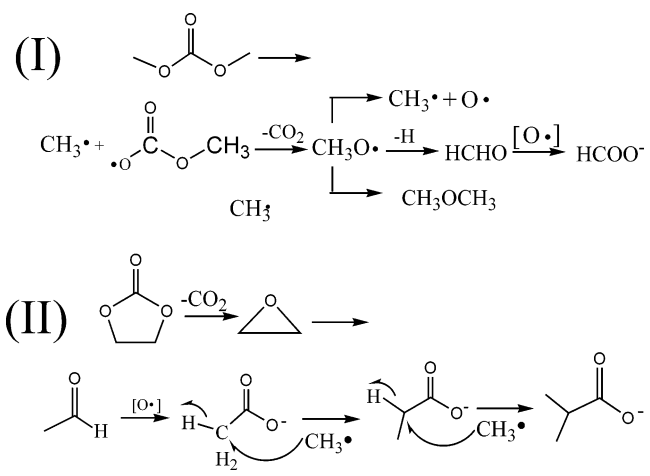

For uncoated $LiNi_{0.8}Co_{0.2}O_2$ electrodes, because of a strong interaction between carboxylate ions and electrode surfaces, the EC intermediates in reaction II, such as CH_3COO^- and $CH_3CH_2COO^-$, are strongly absorbed on electrode surfaces and detected at a high temperature. However, for coated $LiNi_{0.8}Co_{0.2}O_2$ electrodes, these intermediates react with $CH_3\bullet$ to yield the final product $(CH_3)_2CHCOO^-$ because of the weak absorption on the electrode surfaces.

In that work, our experiments have also demonstrated that the decomposition of DMC must undergo an electrochemical oxidation process. Here, according to the tracking experiment on HCHO/$HCOO^-$, we assume that the decomposition of DMC (reaction) may be divided further into two parts as follows

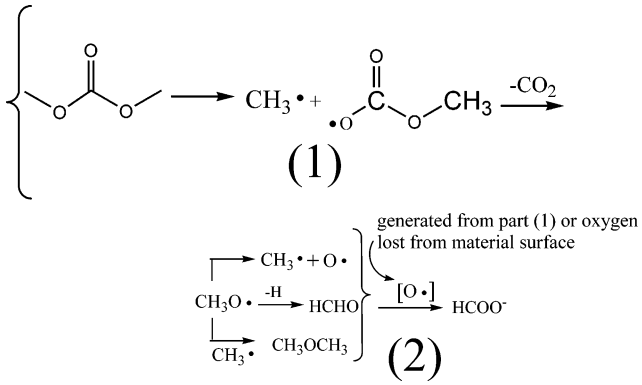

Part 1, the generation of HCHO, is a radical electrooxidation process and is affected by electrode potentials. It is mainly related to the electric field, in addition to transition-metal ion properties. The oxidation to $HCOO^-$ in part 2 may be mainly a chemical process that only depends on the properties of transition-metal ions. Because CH_3CHO and CO_2 have the same *m*/*e* ratio (*m*/*e* = 44), and the amount of CH_3CHO formed is much smaller than that of CO_2, the EC decomposition pattern is difficult to determine experimentally.

The thermal stability of materials closely depends on reactions between materials and electrolytes. The more severely the reaction occurs, the greater the heat that is generated, and that is the source of hazard of lithium-ion batteries. Many experiments have demonstrated that thermal stability in cathode materials is on the order of $LiMn_2O_4$ > $LiCoO_2$ > $LiNi_{0.8}Co_{0.2}O_2$;[20−22] the trend is just opposite to the ease of decomposition in electrolytes on these three cathode surfaces. For $LiNi_{0.8}Co_{0.2}O_2$ electrodes, electrolytes have decomposed extensively at 4.3 V, and many decomposition products are detected (see Table 1 and Figure 7), which means that the reaction between $LiNi_{0.8}Co_{0.2}O_2$ and the electrolytes is severe. In comparison, only a small amount of decomposition products are observed for $LiMn_2O_4$ electrodes even when the potentials are controlled in the range of 3.0−4.6 V, which indicates that reactions between $LiMn_2O_4$ and the electrolytes are limited. Therefore, $LiMn_2O_4$ exhibits the best thermal stability among the three cathode materials. Furthermore, the thermal stability may be further improved by coating, because reactions between cathode materials and electrolytes are further reduced after coating the surfaces with metal oxides. In addition, a study on how a component such as the oxidation products reacts with electrode materials and their thermal behavior in the reaction is being carried out in our laboratory. It will be reported in upcoming papers.

Conclusion

Electrochemical experiments indicate that better cyclic performance could be obtained by coating the cathode material

surface with TiO_2 and that increasing rates of deposition of surface films becomes slower. This is attributed to the presence of TiO_2 on the surface to separate active particles from the organic electrolyte. Electrolyte decomposition on various material surfaces is different; the electrochemical activity of materials follows the decreasing order of $LiNi_{0.8}Co_{0.2}O_2 > LiCoO_2 > LiMn_2O_4$. The causes for the formation of different oxidation products of the electrolytes could be determined by the intrinsic properties of transition-metal ions, including oxidation ability and catalytic activity. The different activities of cathode materials to the oxidation of the electrolytes can well be related to their thermal stability in practical Li-ion batteries.

Acknowledgment. This work was financially supported by the National Natural Science Foundation of China (grants 29925310, 29833090, 20021002). We also thank Prof. Y. L. Chow (Simon Fraser University, Canada) for the comments and discussion of the manuscript.

References and Notes

(1) Shao-Horn, Y.; Weill, F.; Croguennec, L.*Chem. Mater*. **2003**, *15*, 2977−2983.
(2) Shin, Y.; Manthiram, A. *Electrochim. Acta* **2003**, *48*, 3583−3592.
(3) Liu, H. S.; Li, J.; Zhang, Z. R. *J. Solid State Electrochem*. **2003**, *174*, 365−371.
(4) Johnson, C. S.; Kropf, A. J. *Electrochim. Acta* **2002**, *47*, 3187−3194.
(5) Liu, H. S.; Li, J.; Zhang, Z. R. *Electrochim. Acta* **2004**, *49*, 1151−1159.
(6) Ohzuku, T.; Nakura, K.; Aoki, T. *Electrochim. Acta* **1999**, *45*, 151−160.
(7) Pouillerie, C.; Croguennec, L.; Biensan, P. *J. Electrochem. Soc*. **2000**, *147*, 2061−2069.
(8) Croguennec, L.; Suard, E.; Wllmann, P. *Chem. Mater*. **2002**, *14*, 2149−2157.
(9) Cho, J.; Kim, Y. W.; Kim, B. *Angew. Chem., Int. Ed*. **2003**, *42*, 1618−1621.
(10) Chen, Z. H.; Dahn, J. R. *Electrochem. Solid-State Lett*. **2002**, *5*, A213−A216.
(11) Kweon, H. J.; Park, D. G. *Electrochem. Solid-State Lett*. **2000**, *3*, 128−130.
(12) Tarascon, J. M.; Armand, M. *Nature* **2001**, *414*, 359−367.
(13) Oh, S.; Lee, J. K.; Byun, D. *J. Power Sources* **2004**, *132*, 249−255.
(14) Cho, J. *Electrochim. Acta* **2003**, *48*, 2807−2811.
(15) Liu, H. S.; Zhang, Z. R.; Gong, Z. L.;Yang, Y. *Solid State Ionics* **2004**, *166*, 311−325.
(16) Chen, Z. H.; Dahn, J. R. *Electrochem. Solid-State Lett*. **2002**, *5*, A213−A216.
(17) Amatucci, G. G.; Tarascon, J. M.; Klein, L. C. *Solid State Ionics* **1996**, *83*, 167−173.
(18) Zhang, Z. R.; Liu, H. S.; Gong, Z. L.; Yang, Y. *J. Electrochem. Soc*. **2004**, *151*, A599−603.
(19) Zhang, Z. R.; Gong, Z. L.; Liu, H. S.; Yang, Y. *J. Power Sources* **2004**, *129*, 101−106.
(20) Biensan, P. h.; Simon, B.; Peres, J. P.; *J. Power Sources* **1999**, *82*, 906−912.
(21) Zhang, Z.; Fouchard, D.; Rea, J. R. *J. Power Sources* **1998**, *70*, 16−20.
(22) Baba, Y.; Okada, S.; Yamaki, J. *Solid State Ionics* **2002**, *148*, 311−316.
(23) Moshkovic, M.; Cojocaru, M.; Gotttlieb, H. E. *J Electroanal. Chem*. **2001**, *497*, 84−96.
(24) Chebiam, R. V.; Prado, F.; Manthiram, A. *Chem. Mater*. **2001**, *13*, 2951−2957.
(25) Venkatraman, S.; Shin, Y.; Manthiram, A. *Electrochem. Solid-State Lett*. **2003**, *6*, A9−A12.
(26) Levi, M. D.; Salitra, G.; Markovsky, B. *J. Electrochem. Soc*. **2002**, *146*, 1279−1289.
(27) Striebel, K. A.; Sakai, E.; Cairns, E. J. *J. Electrochem. Soc*. **2002**, *149*, A61−A68.
(28) Kanamura, K. *J. Power Sources* **1999**, *81*, 123−129.
(29) Joho, F.; Novak, P. *Electrochim. Acta* **2000**, *45*, 3589−3599.
(30) Ballarin, B.; Seeber, R.; Tonelli, D. *J. Electroanal. Chem*. **1999**, *463*, 123−127.
(31) Manriquez, J.; Bravo, J. L.; Gutierrez-Granados, S. *Anal. Chim. Acta* **1999**, 378, 159−168.
(32) Kowal, A.; Port, S. N.; Nichols, R. J. *Catal. Today* **1997**, *38*, 483−492.
(33) Natile, M. M.; Glisenti, A. *Chem. Mater*. **2002**, *14*, 3090−3099.
(34) Reddy, M. M.; Punniyamurthy, T.; Iqbal, J. *Tetrahedron Lett*. **1995**, *1*, 159−162.